IOP Conf. Series: Materials Science and Engineering **1344** (2026) 012101 doi:10.1088/1757-899X/1344/1/012101

Transient cryogenic thermal management models of liquid hydrogen-fueled electric aircraft

Youngjun Choi[1,2*], Chul H. Kim[1], Peter Cheetham[1,2] and Sastry Pamidi[1,2]

[1] Center for Advanced Power Systems, Florida State University, Tallahassee, FL, USA
[2] Electrical and Computer Engineering Department, FAMU-FSU College of Engineering, Florida State University, Tallahassee, FL, USA

*E-mail: yc25e@fsu.edu

Abstract. A transient cryogenic thermal management model of the electrical power system of the Integrated Zero Emission Electric Aviation (IZEA) conceptual aircraft is described. The aircraft concept uses liquid hydrogen (LH_2) as the heat sink in the primary cooling loop and supercritical helium as the coolant in the secondary cooling loops of superconducting and other power devices. Both LH_2–helium heat exchange and the secondary closed loop helium circulation were modeled. The impact of heat exchanger effectiveness on the required helium mass flow rate in the secondary loops was evaluated for different segments of the aircraft's mission profile. The model components of each device were connected in series to simulate the helium flow control and the target operating temperature of each device under the defined aircraft mission profile. The helium mass flow rate required to maintain the target temperature decreases with increasing heat exchanger efficiency, up to 60% when the heat exchanger effectiveness rises from 0.3 to 0.7. Designing effective heat exchangers is vital because a lower helium flow rate enables the use of smaller impellers, thereby reducing system weight and thermal losses. The models will support the design optimization of the cryogenic thermal management system for the IZEA aircraft.

1. Introduction

As global industrialization and urbanization continue to accelerate, the associated increase in fossil fuel consumption and greenhouse gas (GHG) emissions is driving the progression of climate change [1]. In response, governments and the private sector worldwide are actively seeking effective strategies to decarbonize and reduce GHG emissions. The transportation sector alone accounts for approximately 14% of global carbon emissions [2], making it a critical target for decarbonization efforts.

Electric and hydrogen propulsion technologies have garnered significant attention in recent years due to their potential to substantially reduce emissions compared to conventional fossil-fuel-based transportation. These technologies are being actively developed not only for automobiles but also for aircraft, ships, and trains [3–5]. Green hydrogen produced from renewable energy sources, if widely deployed, will lead to cleaner and more sustainable transportation systems [6].

Among hydrogen storage methods, liquid hydrogen (LH_2) offers significant advantages due to its higher volumetric energy density compared to gaseous hydrogen, enabling more efficient transport and compact storage at relatively low pressures [7, 8]. When LH_2 at 20 K is used as the energy source, its cryogenic cooling power is an advantage for systems that use superconducting devices in cryogenic thermal management [9]. However, hydrogen's high flammability and extremely low ignition energy pose substantial safety risks, particularly when it comes into direct contact with system components. Hence, LH_2 systems commonly employ indirect cooling strategies, utilizing helium in secondary loops for heat transfer from the thermal loads to the LH_2 heat sink [10, 11].

The Integrated Zero-Emission Aviation (IZEA) is a conceptual next-generation hybrid hydrogen-electric platform developed to meet the growing demand for zero emission electric aviation [12]. IZEA incorporates an electric propulsion system using LH_2 as the energy carrier. LH_2 serves a dual purpose: it acts as a high energy density fuel and as a heat sink for various onboard subsystems, including cryogenic superconducting power system components.

IZEA features a highly integrated architecture in which electric motors, generators, power electronics, and energy storage systems are thermally managed via supercritical helium circulation in secondary thermal loops. The configuration enables modular and flexible cooling while eliminating the fire risk associated with direct hydrogen contact.

Efficient use of a limited amount of cooling power in LH_2 carried as an energy source is crucial. Thermal management at the system level must achieve the targets of lightweight, compactness, and reliability, which are essential for electric aircraft. Most existing models focus on steady-state conditions or component-level analyses, limiting their ability to capture the dynamic interactions inherent in an integrated thermal management system. To address this gap, our study developed a transient, system-level cryogenic thermal management model tailored to the IZEA platform.

2. Aircraft overview and mission profile

2.1 Aircraft specifications

The IZEA aircraft is designed to carry approximately 112 passengers, placing it within the size class of current narrow-body commercial airliners. It has a target take-off gross weight (TOGW) of approximately 54.4 metric tons (120,000 lb) and is intended for medium-range missions exceeding 3,700 km (2,000 nautical miles), with a cruise speed of Mach 0.74. This range is sufficient to cover the majority of domestic U.S. routes as well as regional international flights [12, 13].

As illustrated in Fig. 1, the eco-friendly propulsion system comprises two gas turbines, two high-temperature superconducting (HTS) generators rated at 7.5 MW each, sixteen HTS power cables, eight electric motors rated at 2 MW each, and two fuel cell stacks rated at 1 MW each. In addition to the primary propulsion components, the system includes auxiliary subsystems such as motor drives, rectifiers, LH_2 storage tanks, and thermal management units, as well as accommodations for passenger seating and cargo storage.

LH_2 serves both as a coolant for main components and as fuel for the gas turbines and fuel cells. Superconducting applications must be maintained below their critical temperature, and other power components also operate at low temperatures to achieve high efficiency. To generate thrust for both the gas turbines and fuel cells, hydrogen is required to be at room temperature or above. LH_2, with a saturation temperature of 20-23 K depending on storage pressure, is used sequentially to cool devices on board satisfying their temperature requirements and is subsequently delivered to the fuel cells and gas turbines for cooling. As summarized in Table 1,

Table 1. Specification of main components.

Components	Operating temperature [K]	Efficiency corresponding to power rate [%]			
		100 %	70 %	50 %	30 %
Generator	30 ~ 40	99.90	99.86	99.82	99.80
HTS cable	50 ~ 60	99.9			
Motor	110 ~ 140	99.2	99.4	99.5	99.7
Fuel cell	333 ~ 353	48.4	55.0	57.2	61.6

the main components operate under cryogenic conditions, and their efficiencies are considered as a function of their power rates.

2.2 Mission profille and heat load

As shown Fig. 2(a), a generator and fuel cells make power for IZEA. The mission profile is divided into take-off, cruise, and landing phases. During take-off, the highest power is required due to the need for maximum thrust to overcome inertia. The majority of the mission duration is spent in the cruise stage, where a steady power is necessary to maintain the desired speed and altitude, ensuring efficient and stable flight.

The heat loads of main components occur based on the efficiency as shown in Fig. 2(b). To maintain the operating temperature of generator, HTS cable and motor, the heat loads should be removed by the cryogenic fuel, LH_2. Fuel cells can be cooled with water and air because they

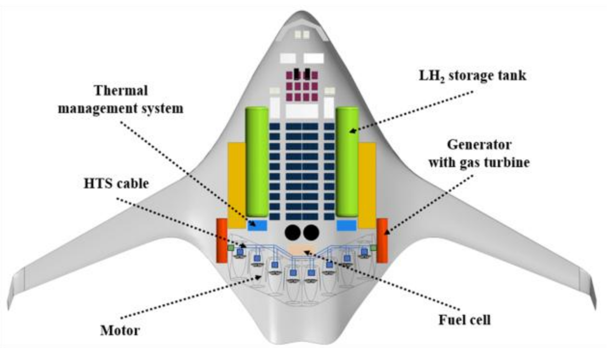

Figure 1. Schematic diagram of IZEA aircraft.

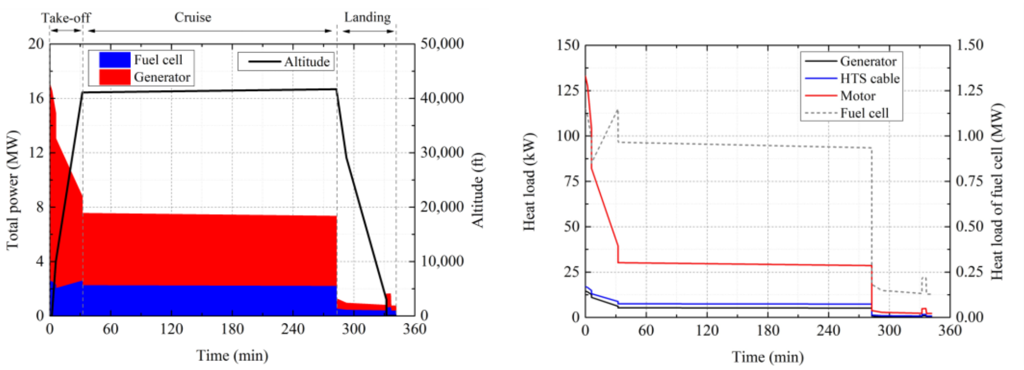

(a) (b)

Figure 2. (a) Total power required and (b) heat loads according to IZEA aircraft mission.

require an operating temperature above room temperature, even though they have higher heat load than other components.

The generator are capable of rapid reponse under viriable operations, whereas fuel cell faces challenges in adopting to load fluctuations due to their slower electrochemical dynamics. Fuel cell only supply power for cruise and auxiliary systems. Generator makes almost power of mission profile. During landing, the generator is operated at minimum power. The required hydrogen for gas turbine and fuel cell was calculated by energy conversion efficiency as discribed in Eq.(1).

$$\dot{m}_{H_2} = \frac{P_{prop}}{\eta_{conv} \times LHV_{H_2}} \quad (1)$$

where $\dot{m}_{H_2}, P_{prop}, \eta_{conv}$ and LHV_{H_2} are mass flow rate of required hydrogen, power, energy conversion efficiency and lower heating value of hydrogen.

Fig. 3(a) shows mass flow rate of hydrogen for fuel cell and gas turbine according to energy conversion efficiency. The latent heat of the saturated liquid hydrogen supplied for cooling the major components, as well as the sensible heat up to the operating temperature, can be utilized. The available cooling heat of the liquid hydrogen supplied to the fuel cell and gas turbine at different temperatures can be seen in Fig. 3(b).

3. Matlab simulation model of thermal management system

3.1 LH_2-Helium heat exchanger and thermal management system model

Thermal management system (TMS) is needed to manage multiple temperature ranges of IZEA components. We designed an integrated heat exchanger, which has a few advantages: minimize heat leaks in heat exchangers, simpler plumbing for LH_2, versatile cooling on each component by secondary and independent flow controls for resilient cooling.

LH_2 cools helium in the main loop and helium is circulated into secondary close loop by fan and cools the components as shown in Fig. 4. Due to its lower condensation temperature compared to hydrogen, helium is well-suited for use as a secondary coolant without phase change.

The power grid on the IZEA aircraft is split into two symmetrical sections. Therefore, one side of the power grid is modeled in TMS that includes one generator, eight HTS cables and four motors. The TMS was modeled on Matlab Simulink platform being capable of simulating transient phenomena. The counterflow-type heat exchanger model is used to estimate heat transfer between LH_2 and helium. Fig. 5(a) shows the unit module of heat exchanger. One helium loop

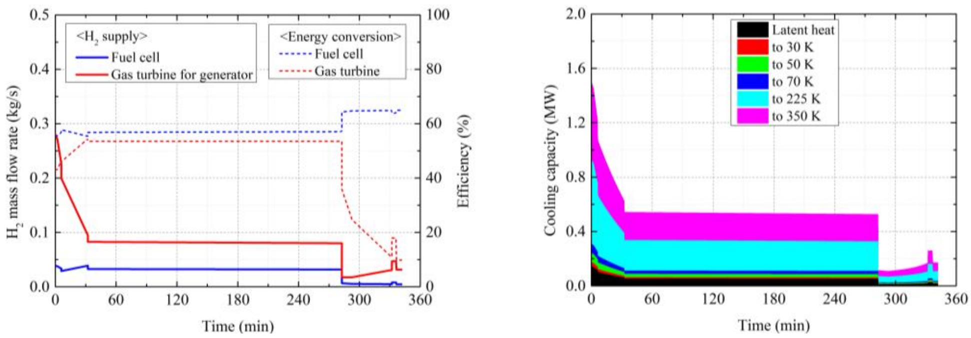

(a) (b)

Figure 3. (a) Total mass flow rate for power output by generator and fuel cell and (b) corresponding cooling power available.

cooled by LH_2 serves the one component to maintain the operating temperature. Balanced with the total pressure drop induced by pipes and the channels in component heat exchanger, helium is circulated by cryo-fan. TMS model is extended from a unit module to a multi-stage configuration as shown in Fig. 5(b). Table 2 summarizes the operating conditions of this simulation.

3.2 Heat exchanger design equations

The effectiveness method was employed for the analysis and design of LH_2-helium heat exchangers as described in Eq.(2)-(4). It is a performance metric used to evaluate how well a heat exchanger transfers heat relative to the maximum possible heat transfer under given conditions. LH_2 absorbs a large amount of heat essentially at constant temperature during a liquid-to-gas phase change.

$$\dot{Q}_{max} = \dot{m}_{He} \times C_{p.He} \times (T_{He.in} - T_{H_2.in}) \tag{2}$$

$$\dot{Q}_{act} = \varepsilon \times \dot{Q}_{max} \tag{3}$$

$$T_{He.out} = T_{He.in} - \dot{Q}_{act}/(\dot{m}_{He} \times C_{p.He}) \tag{4}$$

where $\dot{Q}_{max}$, $\dot{Q}_{act}$, $\dot{m}_{He}$, $C_{p.He}$, $T_{He.in}$, $T_{H_2.in}$, ε, and $T_{He.out}$ are maximum possible heat transfer rate, actual heat transfer rate, mass flow rate of helium, specific heat capacity of helium, helium inlet temperature of heat exchanger, hydrogen inlet temperature of heat exchanger, effectiveness of heat exchanger and helium outlet temperature of heat exchanger, respectively.

The analysis of component cooling using the helium secondary loop was conducted under several assumptions, since the detailed design has not yet been finalized. It was assumed that the heat generated by the components would be removed through ideal heat exchange, while nominal values were applied for pressure drop and fan performance. A more rigorous analysis will be possible once the cooling scheme for each component has been established.

3.3 He control algorithm

According to the mission profile, each component generates a heat load depending on its efficiency. These heat loads are removed by the helium in the secondary loop. If helium mass flow rate is insufficient, the components are not adequately cooled, leading to a rise in their temperature. On the other hand, if the helium flow rate is excessively high, the components are overcooled below their operating temperature, resulting in wasted cooling.

At each time step during the mission, the temperature error is evaluated by comparing the helium outlet temperature of the component with the target operating temperature. If the tolerance condition is not met, the helium mass flow rate is adjusted accordingly. This process is repeated at every time step, allowing dynamic adjustment of the helium mass flow rate to maintain the desired operating temperature throughout the entire mission.

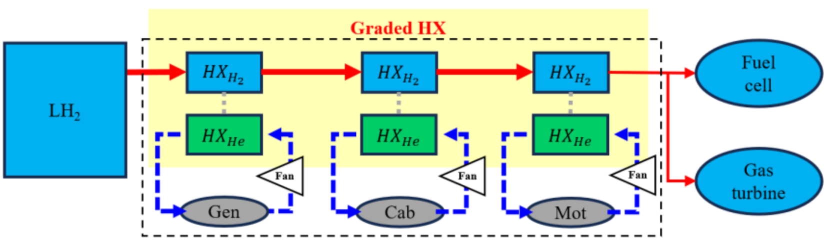

Figure 4. Schematic diagram of cooling loops in TMS.

Table 2. Operating conditions of TMS model.

Parameter	Value	Unit	Parameter	Value	Unit
p_{H_2}	0.15	MPa	$T_{gen.operating}$	35	K
p_{He}	1	MPa	$T_{cab.operating}$	55	K
$\dot{m}_{H_2.initial}$	50	g/s	$T_{mot.operating}$	125	K
$\dot{m}_{He.initial}$	300	g/s	ε	0.3	-

4. Simulation results

After the completion of the initial cooling, the TMS regulates the helium mass flow rates individually for the generator, cable, and motor according to the mission profile, as illustrated in Fig. 6(a). Although each component generates a different heat load, the helium control algorithm effectively maintains their operating temperatures, as seen in Fig. 6(b). According to Fig. 2, during cruise, the generator has a lower heat load than the motor; however, due to its lower operating temperature, it requires a higher helium flow rate, because allowed helium temperature rise (approximately 20 K) from inlet temperature for the generator is smaller than that for motor (approximately 80 K).

The hydrogen after cooling the motor remains relatively cold. Before being supplied to the gas turbine and fuel cell, the hydrogen must be heated up to approximately 350 K. To increase its temperature, the hydrogen is used to cool the fuel cell. Despite this cooling process, the fuel cell still demands a considerable amount of additional cooling, as indicated in Fig. 6(c). This residual heat must be removed through either water or air/skin cooling, leveraging the low ambient air temperatures at high altitude and the aircraft's velocity [14].

In the TMS, each component requires a dedicated fan to circulate helium. The heat loss and weight associated with each fan are dependent on the required helium flow rate. The highest

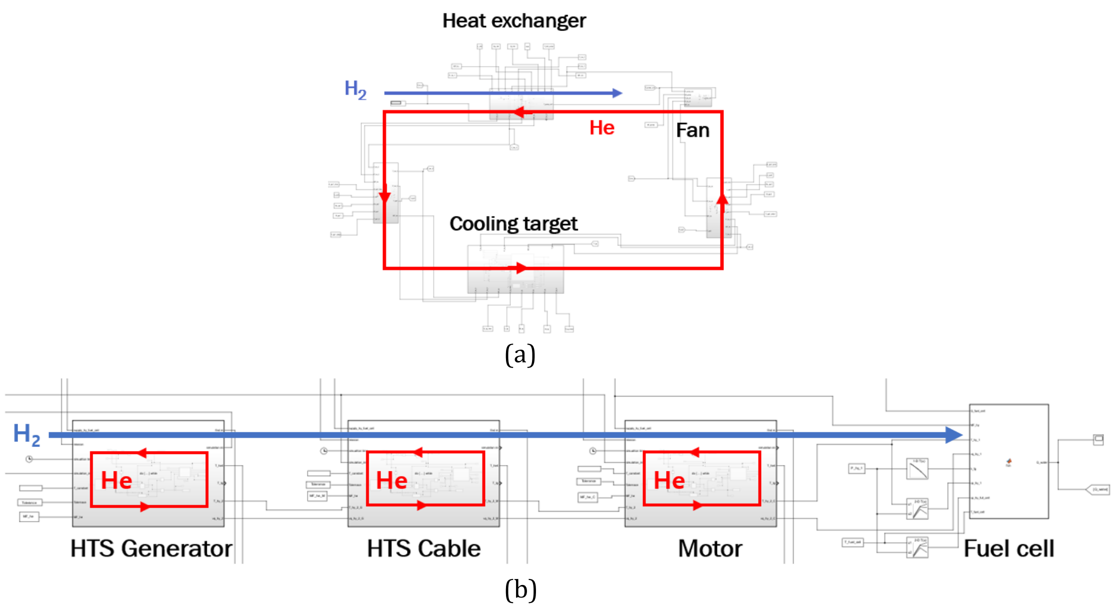

Figure 5. Matlab Simulink model of TMS for (a) a unit cooling and (b) multiple units cooling.

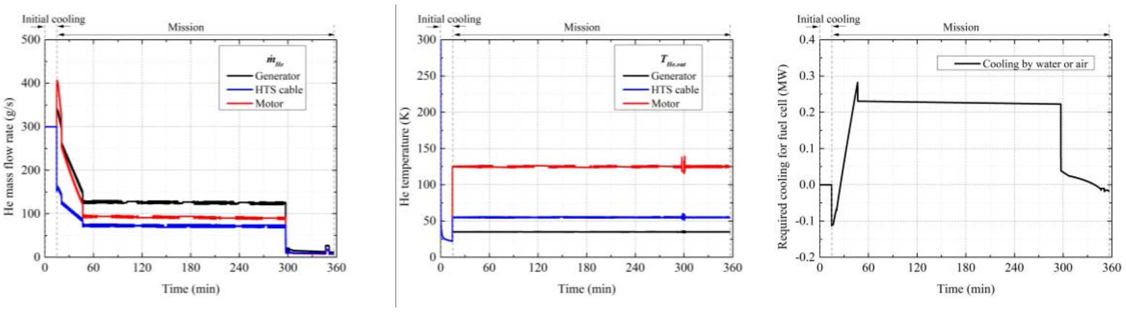

(a) (b) (c)

Figure 6. Simulation result of TMS (a) helium mass flow rate, (b) temperature and (c) required cooling for fuel cell.

Table 3. Helium mass flowrate depending on effectiveness of the graded heat exchanger.

Components	Mass flow rate of helium [g/s]						Ratio of flow rate reduction by improving ε
	Take-off			Cruise			
	ε = 0.3	ε = 0.5	ε = 0.7	ε = 0.3	ε = 0.5	ε = 0.7	
HTS Generator	340	196	136	131	79	56	up to 60.0%
HTS cable	151	88	61	75	46	33	up to 59.6%
Motor	403	238	165	96	59	42	up to 59.1%

helium demand occurs during take-off, which coincides with the peak heat load in the mission profile. However, since the system operates predominantly in cruise, the helium flow rate during cruise is also a key parameter for overall efficiency.

Table 3. presents the required helium flow rates depending on effectiveness of the graded heat exchanger. As the effectiveness increases, the required helium flow to maintain operating temperatures decreases. For example, when the effectiveness increases from ε = 0.3 to 0.7, the required helium flow can be reduced by up to 60% during take-off and by up to 57 % during cruise. Therefore, employing high-effectiveness heat exchangers reduces fan loading significantly and contributes to improved overall system efficiency.

5. Conclusion

A transient cryogenic thermal management model of the electrical power system of the Integrated Zero Emission Electric Aviation conceptual aircraft was developed to evaluate component-level heat exchangers of varying effectiveness. The aircraft concept uses LH_2 as the heat sink in the primary cooling loop and supercritical helium as the coolant in the secondary cooling loops of superconducting and other power devices. The model simulates both LH_2–helium heat exchange and secondary closed-loop helium circulation, incorporating the effectiveness of the heat exchanger. The model components of each device were connected in series to simulate the helium flow control and temperature maintenance of each component under the defined aircraft mission profile.

The required helium mass flow rate for component device cooling decreases as the heat exchanger effectiveness increases. A lower helium flow rate enables the use of smaller impellers, which reduces system weight and minimizes thermal losses due to fan power consumption, thereby improving overall system efficiency. When the effectiveness increases from 0.3 to 0.7, the

Table 4. Specification of various cryogenic fans made by Stirling Cryogenics [15].

Model	Mistral	Noorden-wind	Bize	Neyol	Nodin	Tramont-ana	Yeti
Motor power [W]	5	80	340	340	340	2400	3600
Impeller [mm]	20	31	56	75	85	140	240
Flow[m^3/hr]	0.07	1.85	7.6	34	45	300	500
Weight [kg]	3	3	18	18	18	90	157

flow of helium needed is lowered by up to 60%. Table 4 summarizes the specifications of cryogenic fans from Stirling Cryogenics. Based on fitted correlation of fan mass with flow rate, the fan weight is found to decrease from 350 kg to 160 kg, as the heat exchanger effectiveness improves [13,15]. The simulation model developed is intended to support the design and optimization of the thermal management system for the IZEA aircraft.

Acknowledgments

This work was supported by the Office of Naval Research (ONR) under grant number N000141612956 and NASA University Leadership Initiative (ULI) #80NSSC22M0068

References

[1] IEA, CO2 Emissions in 2022. Accessed on: June. 6, 2025, [Online]. Available: https://www.iea.org/reports/co2-emissions-in-2022
[2] EPA, Global Greenhouse Gas Emissions Data. Accessed on: June. 6, 2025, [Online]. Available: https://www.epa.gov/ghgemissions/global-greenhouse-gas-emissions-data
[3] Shakeri N, Mehdi Z, and Jorgen N. "Hydrogen fuel cells for ship electric propulsion: Moving toward greener ships." IEEE Electrification Magazine 8.2 (2020): 27-43.
[4] Hoffrichter A, Stuart H, and Clive R. "Conceptual propulsion system design for a hydrogen-powered regional train." IET Electrical Systems in Transportation 6.2 (2016): 56-66.
[5] da Silva F, Fernandes J, and Branco P. "Barriers and challenges going from conventional to cryogenic superconducting propulsion for hybrid and all-electric aircrafts." Energies 14.21 (2021): 6861.
[6] Oliveira A, Beswick R, and Yan Y. "A green hydrogen economy for a renewable energy society." *Current Opinion in Chemical Engineering* 33 (2021): 100701.
[7] Wu J, Chen S, Yu M, Zhang X and Jiang L. "Techno-economic analysis on low-temperature and high-pressure cryo-adsorption hydrogen storage." Fuel 381 (2025): 133532.
[8] Wang H, Zhao Y, Dong X, Yang J, Guo H, and Gong M. "Thermodynamic analysis of low-temperature and high-pressure (cryo-compressed) hydrogen storage processes cooled by mixed-refrigerants." International Journal of Hydrogen Energy 47.67 (2022): 28932-28944.
[9] Hara S, Iwami Y, Kawasaki R, Matsumoto T, Shirai Y and Shiotsu M. "Development of liquid hydrogen cooling system for a rotor of superconducting generator." *IEEE Transactions on Applied Superconductivity* 31.5 (2021): 1-5.
[10] Nam G, Sung H, Ha D, No H, Koo T, Ko R and Park M. "Design and analysis of cryogenic cooling system for electric propulsion system using liquid hydrogen." Energies 16.1 (2023): 527.
[11] Cirrone D, Makarov D, Proust C and Molkov V. "Minimum ignition energy of hydrogen-air mixtures at ambient and cryogenic temperatures." international journal of hydrogen energy 48.43 (2023): 16530-16544.
[12] Gladin J, Paatel S, Ahuja J and Mavris D. "Near zero emissions flight enabled by a robust hybrid-electric architecture." AIAA Aviation Forum and Ascend 2024. 2024.
[13] Virdi P. et al. "Liquid hydrogen storage, thermal management, and transfer-control system for integrated zero emission aviation (IZEA)." *Applied Energy* 393 (2025): 126054.
[14] Guo J, Zheng J, Gladin J, Ordonez J, Cooley L and Cattafesta L. "Challenges in Cooling Required for Fuel Cells in Aviation Applications." AIAA AVIATION FORUM AND ASCEND 2024. 2024.
[15] Stirlingcryogenics, Accessed on: Sep. 15,2025 [Online]. Available: https://stirlingcryogenics.com/products/cryogenic-fans/